Memoirs of the Faculty of Engineering
Fukuyama University
No. 2, March 1980

ULTIMATE STRENGTH OF BEAMS WITH HOLES IN HIGH SHEAR

Minoru UENOYA*

Introduction

Ultimate strengrh of steel beams with web holes has recieved considerable attention in recent years, and a number of publications have described the elastic stress analysis and ultimate strength of beams with or without reinforcement. Much of the research concerning web holes has been reviewed in reference (1).

Herein attention is restricted to the ultimate strength of wide flange beams with unreinforced web holes. For predicting the ultimate strength of the beam, several methods have been proposed in which the effects of shear and normal force on the plastic moment were considered. Bower[2,3] gave a lower bound solution in which equilibrium was satisfied and points of contraflexure in the tee-sections above and below the hole at the midpoint of the hole were assumed. Redwood[4] assumed different stress distributions at both high and low moment ends of the hole. These two methods lead to similar results and generally are conservative when the shear to moment ratio is high.

This investigation extends the ultimate strength analysis by including consideration of the shear force carried by the flange in the tee-section, and compares the predictions with the results of beam tests carried out under various loading conditions and with different sizes of holes.

---

* Department of Civil Engineering

Analysis

Plastic analysis is based on the theory of plastic collapse in which material behavior is assumed perfectly plastic. The hole to be analysed is located at middepth of beam web and is symmetric about horizontal and vertical axes. At collapse, hinges are assumed, two located at section 1 and two at section 2 as shown on Fig. 1(a). Stress distributions are also assumed at these locations, both shear and normal stresses being included. When bending moment M and shear force V are acting at the center section of the hole, the shear force is assumed equally distuributed between the upper and lower tee-sections as shown on Fig. 1(b). This is based on the assumption that the points of contraflexure due to shear occur at the midpoint of the hole. At the section 1 and 2 on Fig. 1(b), there are local bending moments, called Vierendeel moments, due to the shear V/2 in addition to the bending moment M.

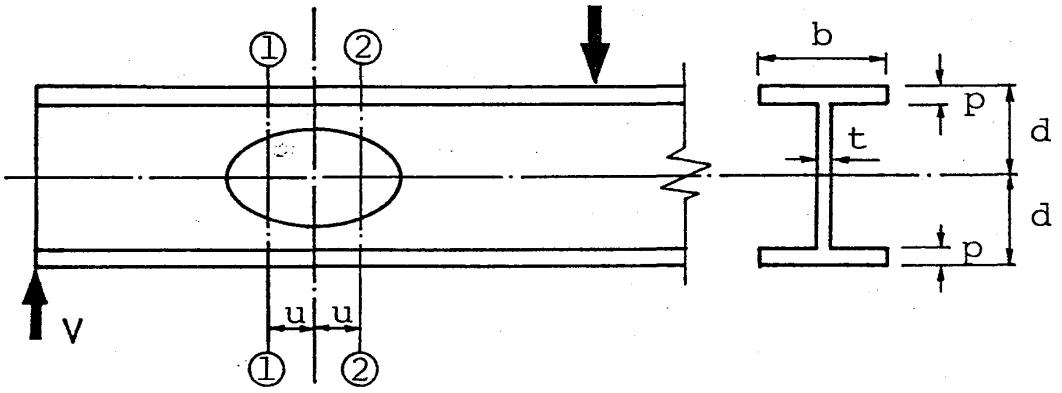

(a) Plastic Hinge Locations

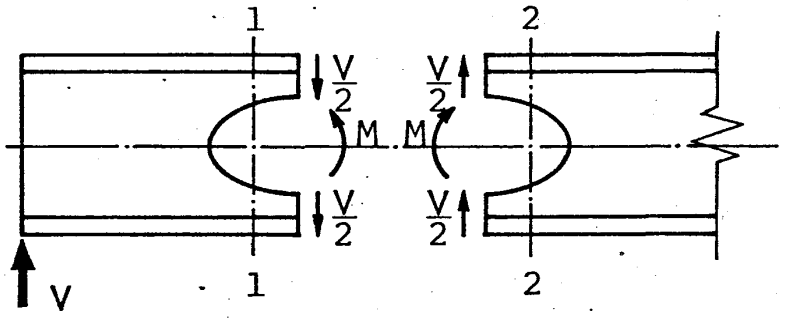

(b) Stress Resultants at Center of Hole

Fig. 1 Plastic Hinge Locations and Stress Resultants

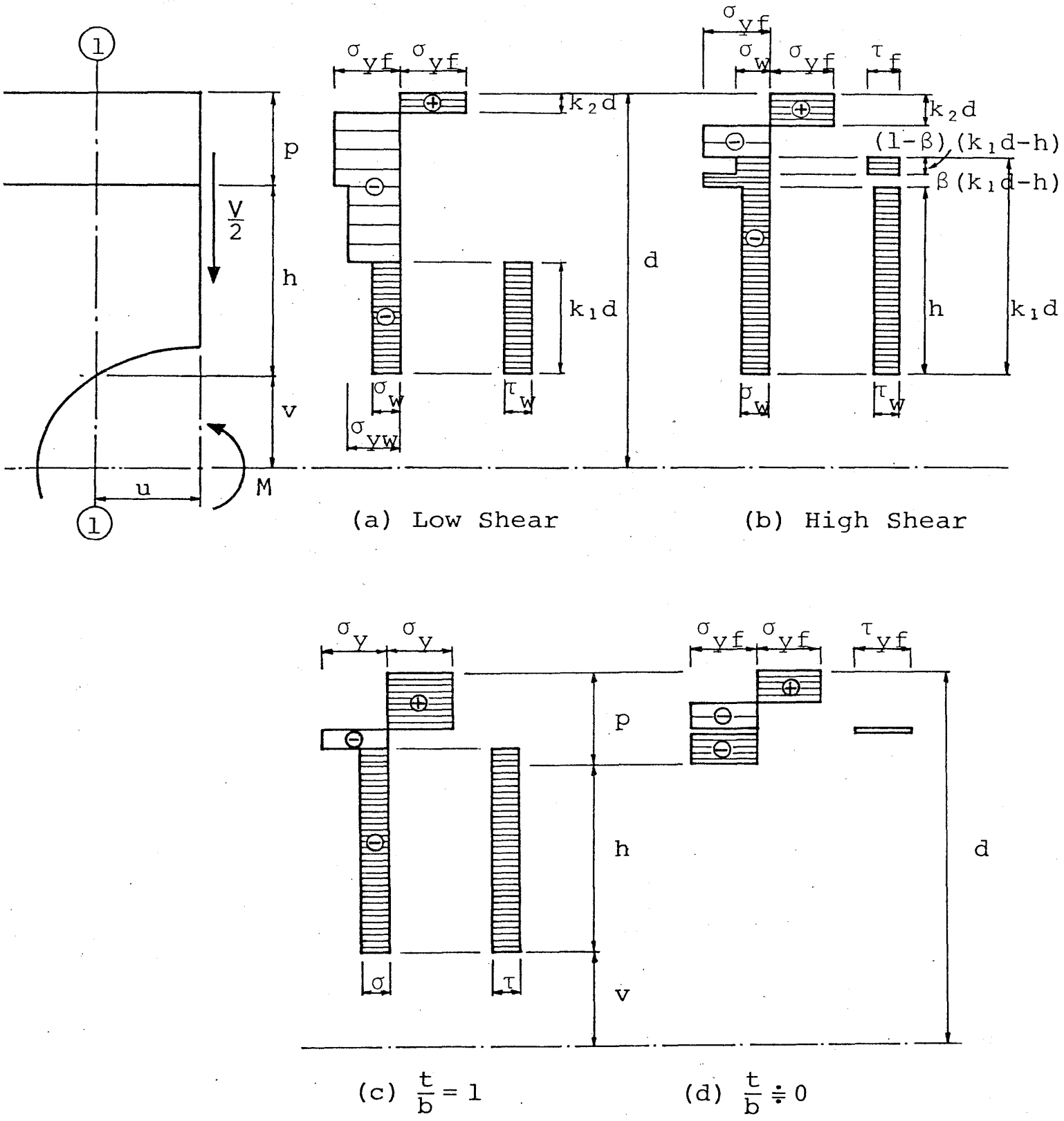

Fig. 2 Stress Distributions at Plastic Hinge for Low Moment

Stress Distibution in Low Shear -- When the shear force is low, the normal and shear stress distributions assumed at section 1 are shown in Fig. 2(a). At section 2, the same stress distributions are assumed except that the sign of the local bending stresses is reversed. These stress distributions are identical to those assumed by Bower[3]. It is assumed that the steel yields according to von Mises yield criterion, hence in the web

$$\sigma_{yw}^2 = \sigma_w^2 + 3\,\tau_w^2 \tag{1}$$

where σ_{yw}, σ_w and τ_w are the yield stress, normal stress and shear stress in the web respectively.

The stress distributions assumed at section 1 are statically equivalent to the stress resultants, hence

$$M = \sigma_{yf}\, b(p-k_2d)[(2-k_2)d-p] + \sigma_{yw}t(h-k_1d)[(2+k_1)d-2p-h] \tag{2}$$

$$V = 2\tau_w\, t\, k_1 d \tag{3}$$

$$\frac{1}{2} V u = \sigma_{yf}\, b\, k_2 d\left[\frac{1}{2}(2-k_1-k_2)d - v\right] \tag{4}$$

$$\sigma_w\, t\, k_1 d = \sigma_{yf}\, b\, k_2 d \tag{5}$$

where σ_{yf} is the yield stress in the flange and the other symbols are defined in Fig. 2(a).

Eliminating V, σ_w and τ_w from Eq. 3 to 5,

$$\frac{1}{4} k_2^4 - \left(1 - \frac{v}{d} - \frac{k_1}{2}\right) k_2^3 + \left[\left(1 - \frac{v}{d} - \frac{k_1}{2}\right)^2 + \frac{1}{3}\left(\frac{u}{d}\right)^2\right] k_2^2 - \frac{1}{3}\left(\frac{1}{\alpha}\right)^2 \left(\frac{t}{b}\right)\left(\frac{u}{d}\right)^2 k_1^2 = 0 \tag{6}$$

where

$$\alpha = \frac{\sigma_{yf}}{\sigma_{yw}} \tag{7}$$

In order to obtain a solution of these equations, a value of k_1 is assumed, k_2 is then obtained from Eq. 6 and hence the corresponding bending moment M and shear force V can be obtained. The relationship between the bending moment M and the shear force V can be presented on interaction diagrams based upon the nondimensional parameters M/M_p and V/V_p. The term M_p is the full plastic moment of the gross beam section as follows;

$$M_p = \sigma_{yf}\, b\, p\, (2d - p) + \sigma_{yw}\, t\, (d - p)^2 \tag{8}$$

and V_p is defined as the yield capacity of the gross beam section as follows;

$$V_p = \frac{2}{\sqrt{3}} [\, \sigma_{yf}\, b\, p + \sigma_{yw}\, t\, (d - p)] \tag{9}$$

Stress Distibution in High Shear -- When the shear force V increases, $k_1 d$ shown in Fig. 2(a) finally reaches the full web height h at section 1. After $k_1 d$ reaches h, Bower assumed that no more shear force can be carried in the section. The stress distributions assumed by Redwood allow a little more shear force untill the full web height yields under the shear stress only.

Herein it is assumed that a part of the flange can carry some shear force; i.e. the value of $k_1 d$ can be larger than the web height h as shown on Fig. 2(b). Since the shear stresses are zero on the surface of the flange except at the interface of web and flange, it is assumed that a portion of the flange, $\beta(k_1 d - h)$ shown in Fig. 2(b), yields at the normal stress σ_{yf} and the remaining portion, $(1-\beta)(k_1 d - h)$, yields according to the yield criterion under the action of the normal stress σ_f and the shear stress τ_f. The nondimensional parameter β introduced herein is assumed a variable with respect to the flange width and the web thickness. When

the flange width b is equal to the web thickness t, the parameter must be zero in order that stress distributions correspond to those of rectangular section beam shown Fig. 2(c). When the flange width b is infinitely wide, the web portion can be neglected and the stress distributions become those of a plate shown Fig. 2(d). Therefore the parameter β is approximately equal to unity. In this report, three curves are proposed for the parameter β and the applicability of these curves is subsequently discussed after comparison with experimental results.

In the case of high shear, with these assumptions, equations 2, 3, 4 and 5 become

$$M = \sigma_{yf} b[(1-k_1-k_2)d-v][(1+k_1-k_2)d+v] \tag{10}$$

$$V = 2\tau_f b(1-\beta)(k_1 d-h)+2\tau_w th \tag{11}$$

$$\frac{1}{2}Vu = \frac{1}{2}\sigma_{yf} bk_2 d(2-k_2)d-\frac{1}{2}\sigma_w th(d-p+v)-\frac{1}{2}\sigma_f b(1-\beta)(k_1 d-h)[2(v+k_1 d)$$
$$-(1-\beta)(k_1 d-h)]-\frac{1}{2}\sigma_{yf} b\beta(k_1 d-h)[2(d-p)+\beta(k_1 d-h)] \tag{12}$$

$$\sigma_{yf} bk_2 d = \sigma_f b(1-\beta)(k_1 d-h)+\sigma_{yf} b\beta(k_1 d-h)+\sigma_w th \tag{13}$$

It is now assumed that

$$\frac{\tau_f}{\tau_w} = \alpha \tag{14}$$

and from Eqs. 1 and 7 it follows that $\sigma_f/\sigma_w = \alpha$ also.

Eliminating V, σ_w, τ_w, σ_f, and τ_f from Eqs. 11to 13 gives

$$\frac{1}{4}k_2^4 - c_3 k_2^3 + \left[c_3^2 - c_4 + \frac{1}{3}\left(\frac{u}{d}\right)^2 \right] k_2^2 + 2\left[c_3 c_4 - \frac{1}{3}\beta\left(\frac{k_1 d - h}{d}\right)\left(\frac{u}{d}\right)^2 \right] k_2$$

$$+ \frac{1}{3}\beta^2 \left(\frac{k_1 d - h}{d}\right)^2 \left(\frac{u}{d}\right)^2 + c_4^2 - \frac{1}{3}\left(\frac{c_1}{\alpha}\right)^2 \left(\frac{u}{b}\right)^2 = 0 \qquad (15)$$

where

$$c_1 = \alpha(1-\beta)\left(\frac{k_1 d - h}{d}\right)\left(\frac{b}{d}\right) + \left(\frac{h}{d}\right)\left(\frac{t}{d}\right) \qquad (16)$$

$$c_2 = \alpha(1-\beta)\left(\frac{k_1 d - h}{d}\right)\left(\frac{b}{d}\right)\left[\frac{v}{d} + k_1 - \frac{1}{2}(1-\beta)\left(\frac{k_1 d - h}{d}\right)\right] + \frac{1}{2}\left(\frac{t}{d}\right)\left(\frac{h}{d}\right)\left(1 + \frac{v}{d} - \frac{p}{d}\right) \qquad (17)$$

$$c_3 = 1 - \frac{c_2}{c_1} \qquad (18)$$

$$c_4 = \beta\left(\frac{k_1 d - h}{d}\right)\left[\frac{p}{d} - \frac{1}{2}\beta\left(\frac{k_1 d - h}{d}\right) - c_3\right] \qquad (19)$$

Experiments

Beam tests were carried out to investigate expermentally the effects of the shear to moment ratio and size of the circular hole on the strength of a beam. A single rolled wide flange beam made of mild steel was cut to provide the test beams. The average value of the dimensions and the material properties are given in Fig. 3 because the variation of these values was very small. Three tensile coupons were prepared from both the flange and the web. Since test beams were annealed in order to remove residual stresses, the difference between tensile yield stresses in the flange and the web is small as shown in Fig. 3. The circular holes were cut by machine.

Four cases of loading were tested shown in Fig. 3 in which Test No. 1 is pure bending, Test No. 2 is low shear, Test No. 3 is

high shear and Test No. 4 is pure shear at the center of the circular hole. Two or three beams were tested in each loading case and sizes of circular holes corresponded to ratios of radius to half depth of beam, r/d, equal to 0.3 and 0.5.

Because the tests were conducted to determine the ultimate strength of beams at the location of the hole, it was necessary to add bearing stiffeners at the reactions and load points and cover plates on the top and bottom flanges of the beams in regions of high moment, so that failure would occur at the hole rather than at some other location.

Dial gages with a least reading of 0.01 mm (0.000394 in.) were placed beneath the beams at the concentrated load and at the center of the hole. Loads were applied to the beam by 200,000 kg (422 kip) capacity Amsler type testing machine in increments of 2000 kg (4.42 kip) in the elastic range and in increments of 500 kg (1.10 kip) after yielding had begun. In the inelastic range, all plastic flow was allowed to take place at each load increment before readings were taken. Typical load-deflection curves obtained from the beam tests are shown in Fig. 4 in which the bending moment at the center of the holes is plotted against the deflection in Tests 1 and 2 and the shear force versus deflection for Tests 3 and 4. The failure load of the beams was determined by the intersection of linear parts of the load-deflection curves as shown on the figure. When the linear inelastic curve was not evident, a line of 1/30 times the slope of the elastic line was drawn tangent to the inelastic part of the curve as used in reference (5). Typical beams after collapse are shown on Fig. 5.

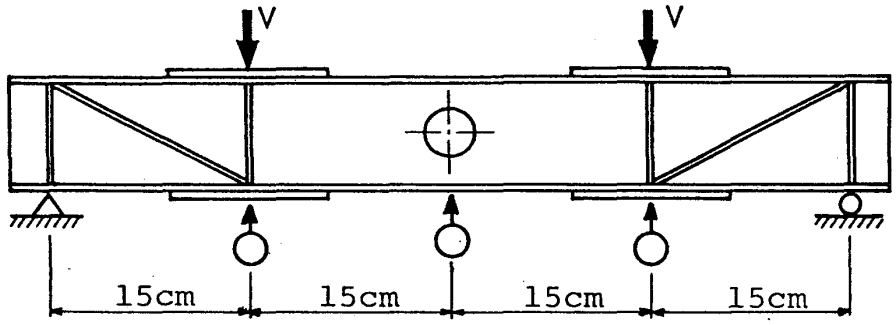

Test No. 1

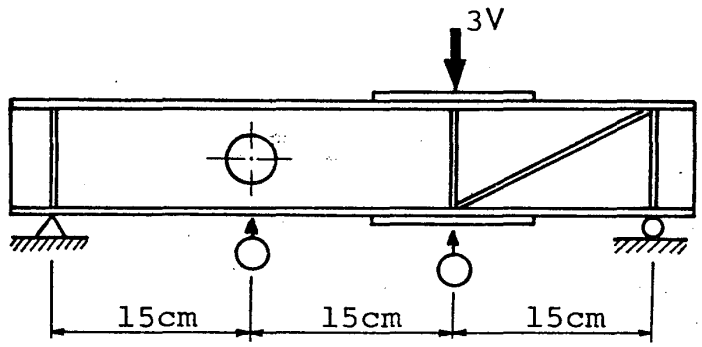

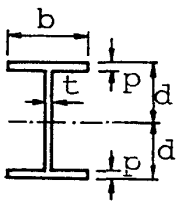

d	5.08cm
b	5.19cm
p	0.64cm
t	0.51cm
σ_{yf}	2580. kg/cm^2
σ_{yw}	2620. kg/cm^2

Test No. 2

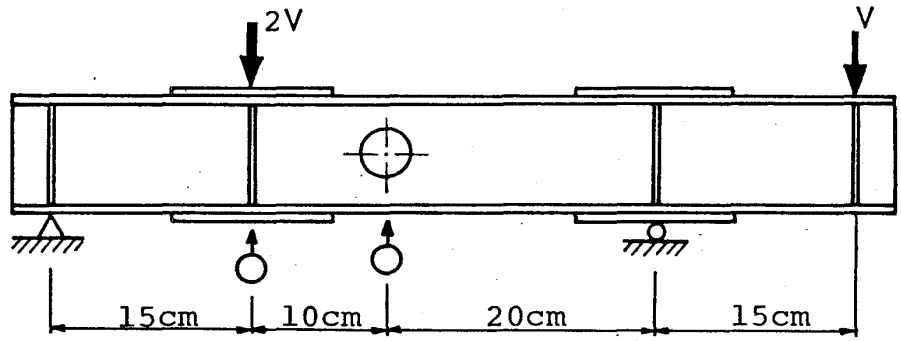

Test No. 3

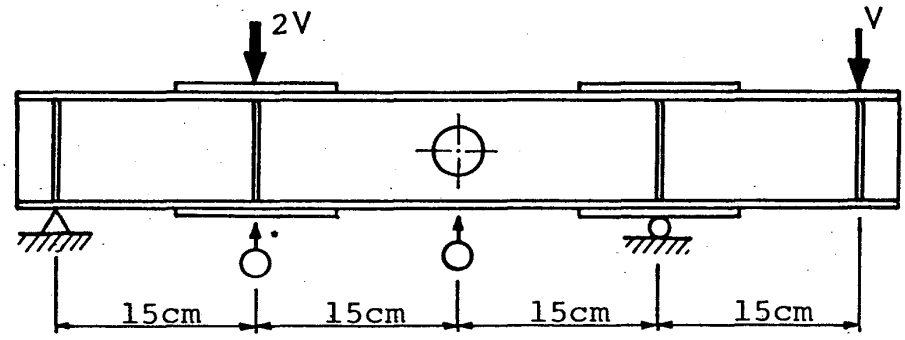

Test No. 4

Fig. 3 Loading Configurations(1 cm = 0.3937 in.; 1 kg/cm^2= 14.21 psi)

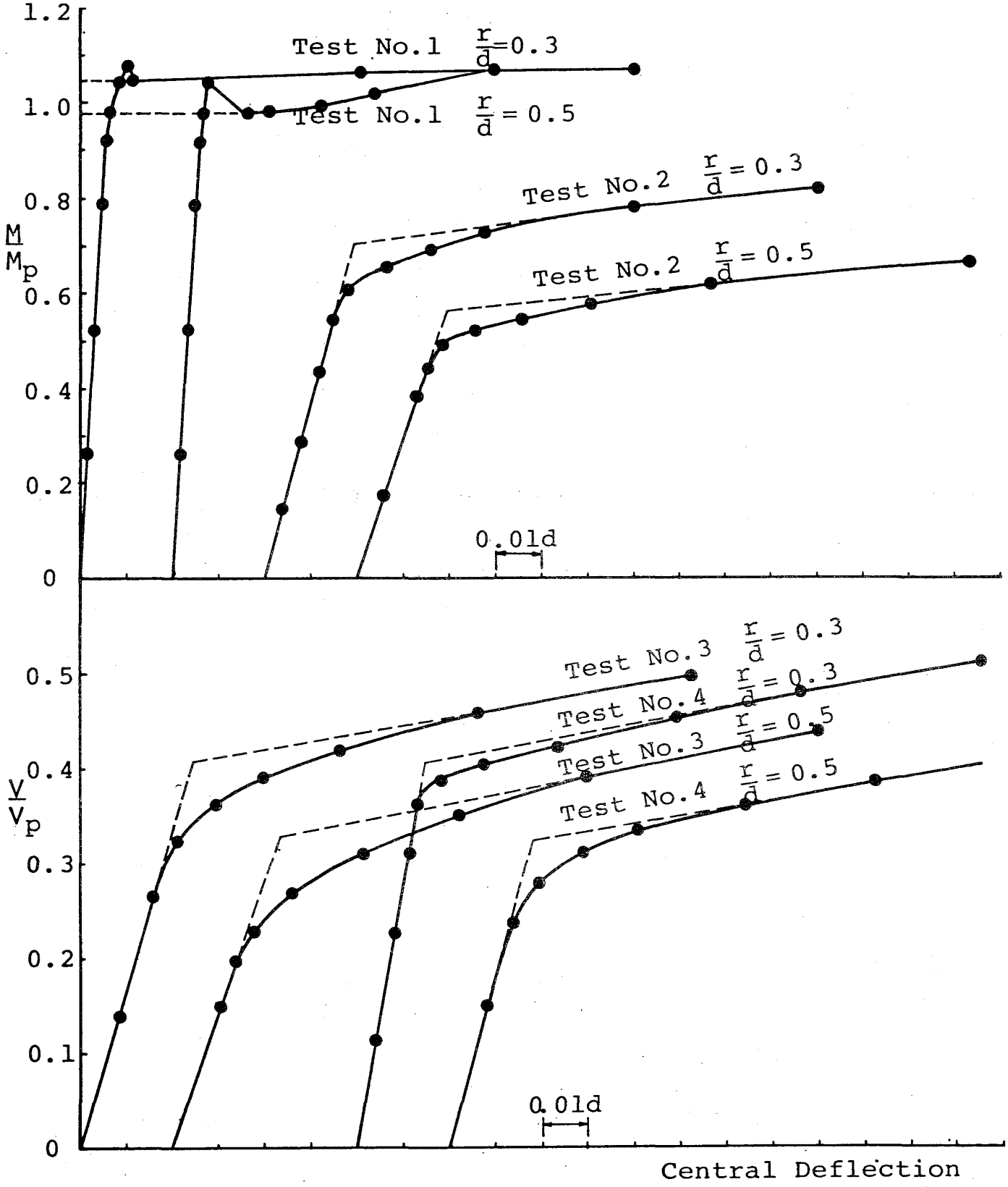

Fig. 4 Measured Deflections at Center of Circular Hole

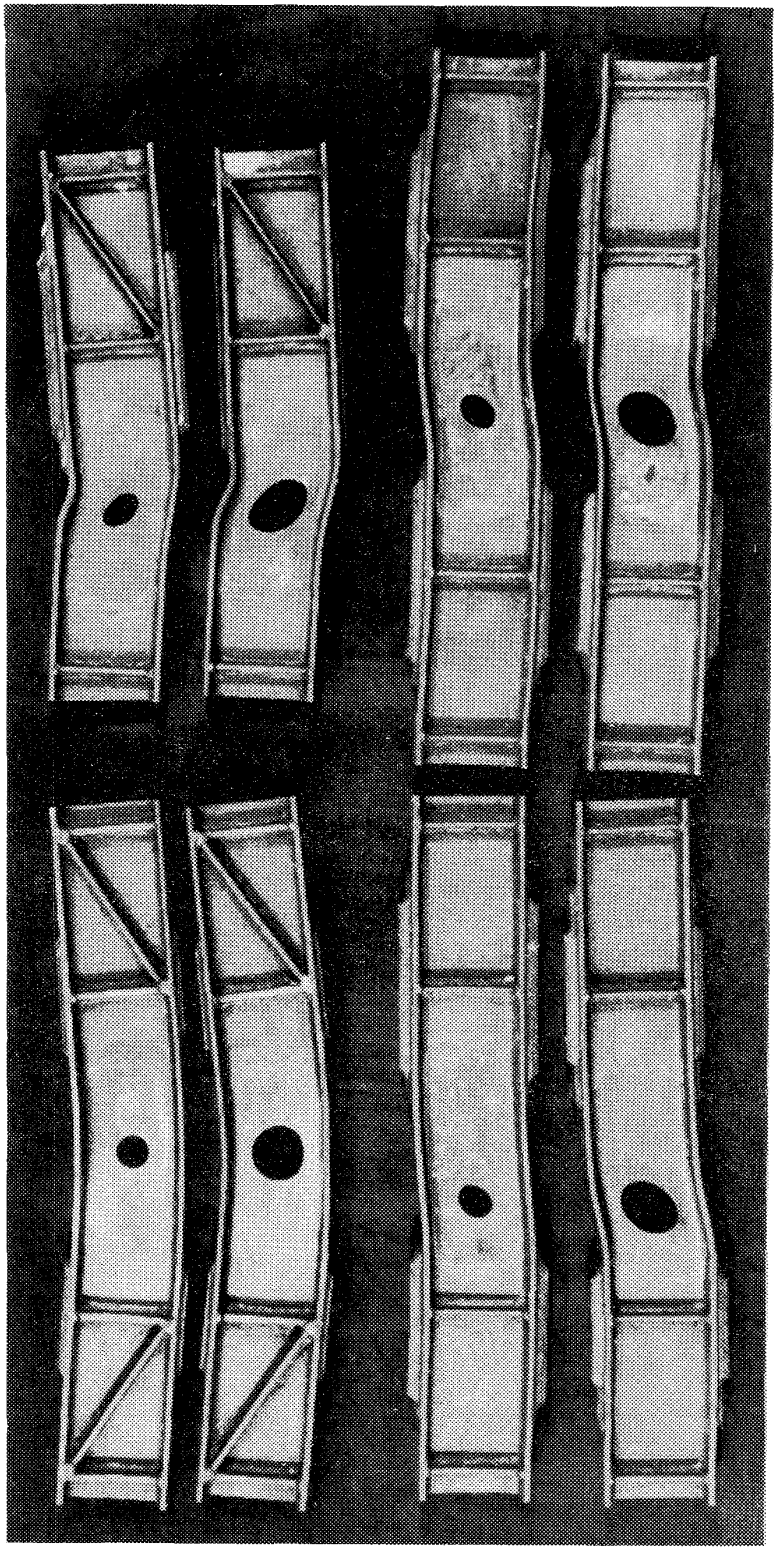

fig. 5 Typical Beams after Collapse

Comparison of analysis and test results

To obtain the theoretical solution, three expressions for the parameter β, all of which satisfy the conditions previously described, are considered as shown in Fig. 6. The three curves in the figure are given by the following:

$$\beta = 1 - \left(\frac{t}{b}\right)^{\frac{1}{2}} \tag{20}$$

$$\beta = 1 - \left(\frac{t}{b}\right)^{\frac{1}{3}} \tag{21}$$

$$\beta = 1 - \left(\frac{t}{b}\right)^{\frac{1}{4}} \tag{22}$$

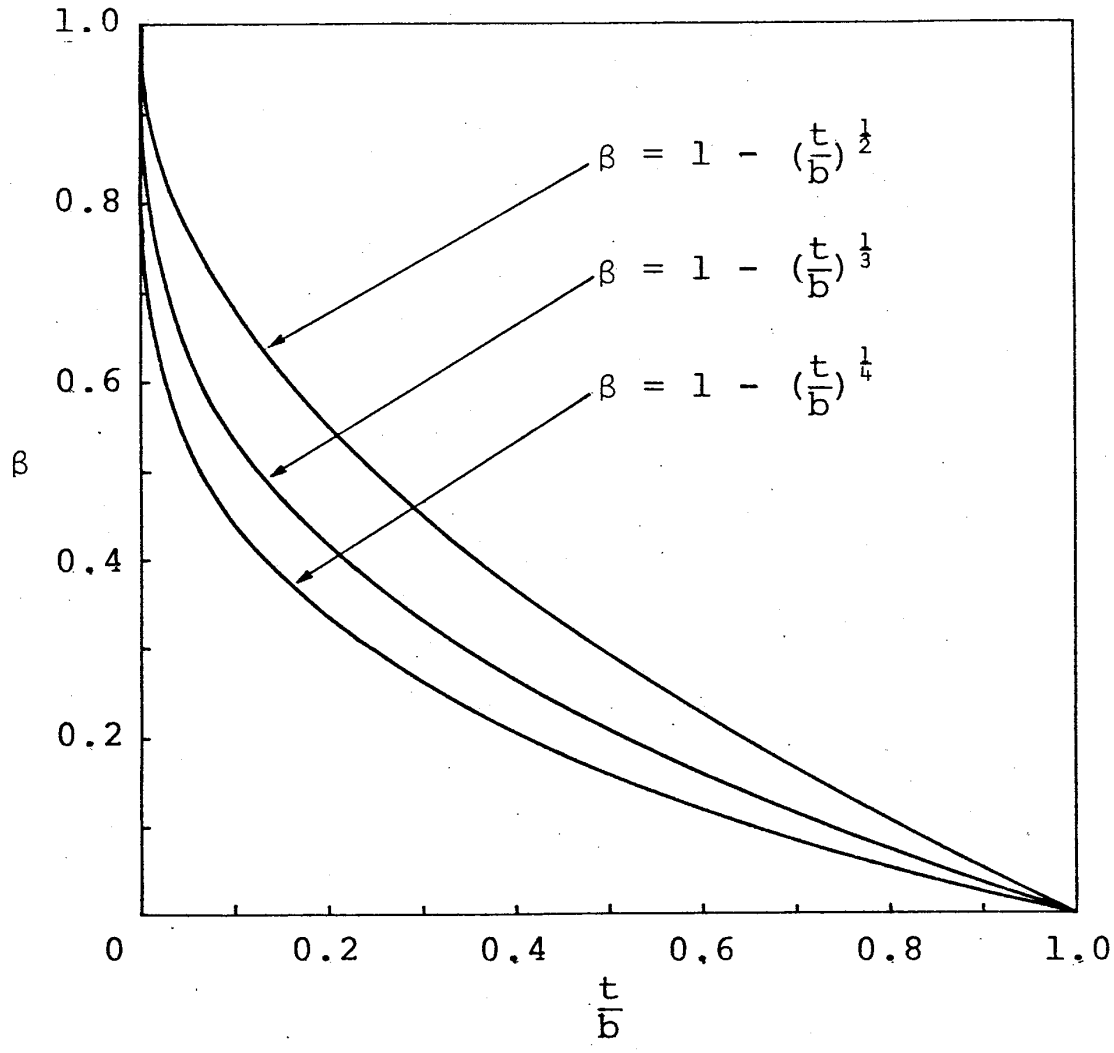

Fig. 6 Assumed Relationships between Parameter β and t/b

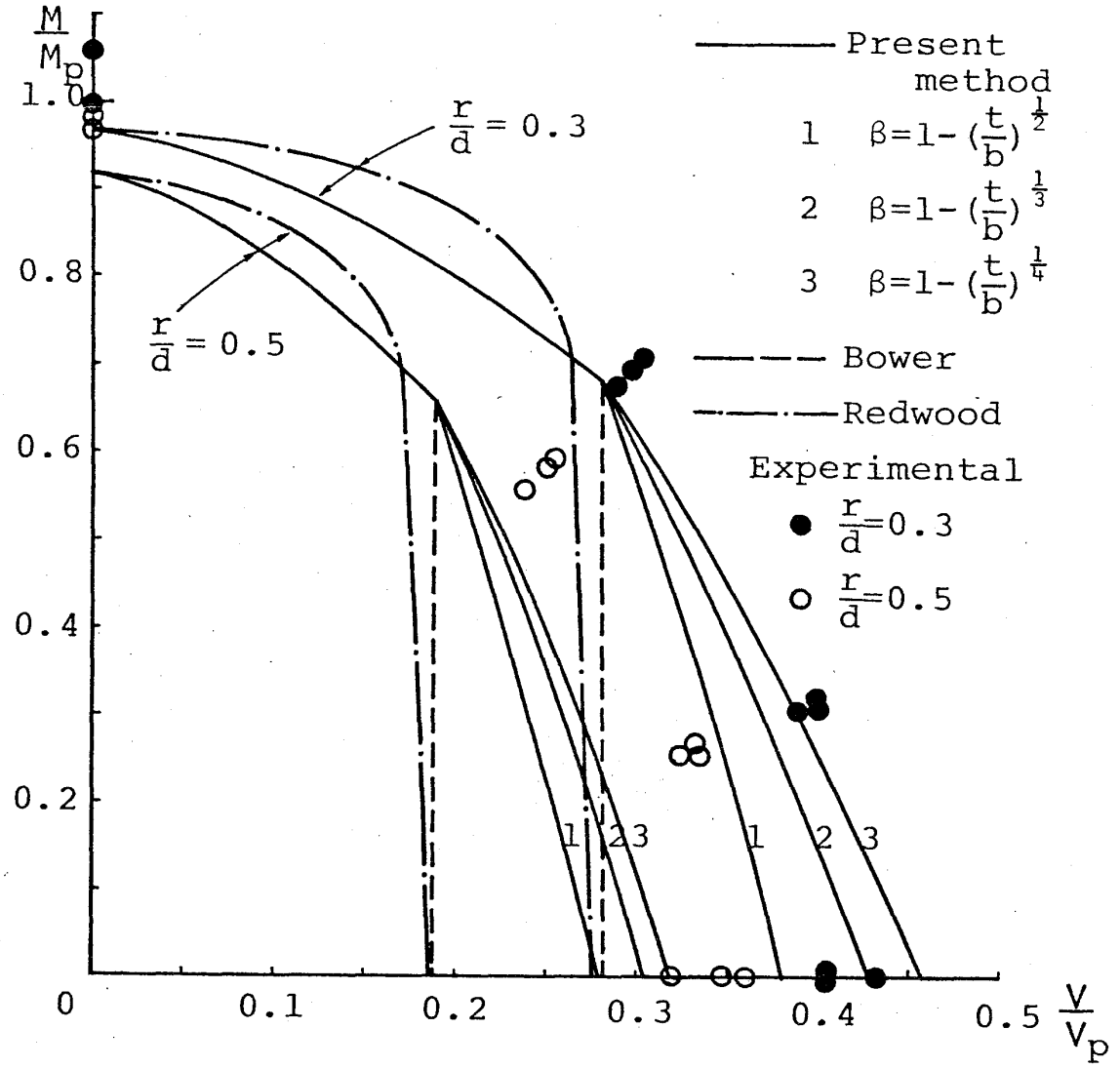

Fig. 7 Interaction Curves for Test Beams with Circular Holes

By using the parameter β defined above, the interaction diagrams for the test beams are shown in Fig. 7. Three theoretical results are given by the present method and two by Bower's[3] and Redwood's[4] methods respectively, and test results are also plotted. Comparing the present method with the experimental results at the high shear to moment ratio, the theoretical results of the present method are slightly conservative when compared with the experimental values, but the both Bower's and Redwood's methods show considerably more conservatism. For the parameter β, Eq.22, the curve 3 in Fig. 7, shows better agreement than the other two, Eqs. 20 and 21. The theoretical failure loads given by the present method using

Eq. 22 are from 2.4 % to 16.4 % smaller than the average of the experimental values except in the case of Test No. 4 with r/d = 0.3, which is 9.4 % greater than the experimental value.

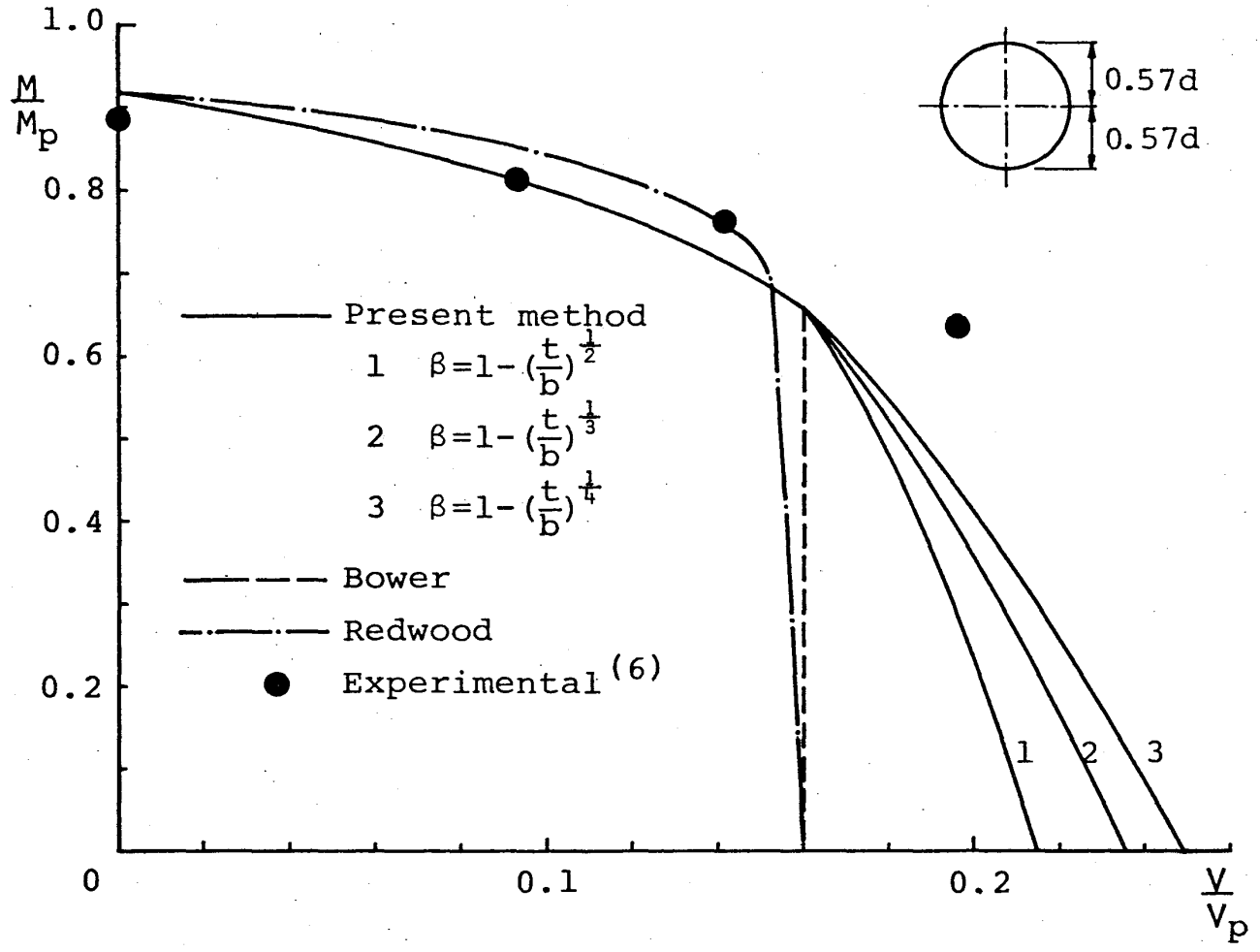

Fig. 8 Interaction Curves for Beams with Circular Holes in Reference(6)

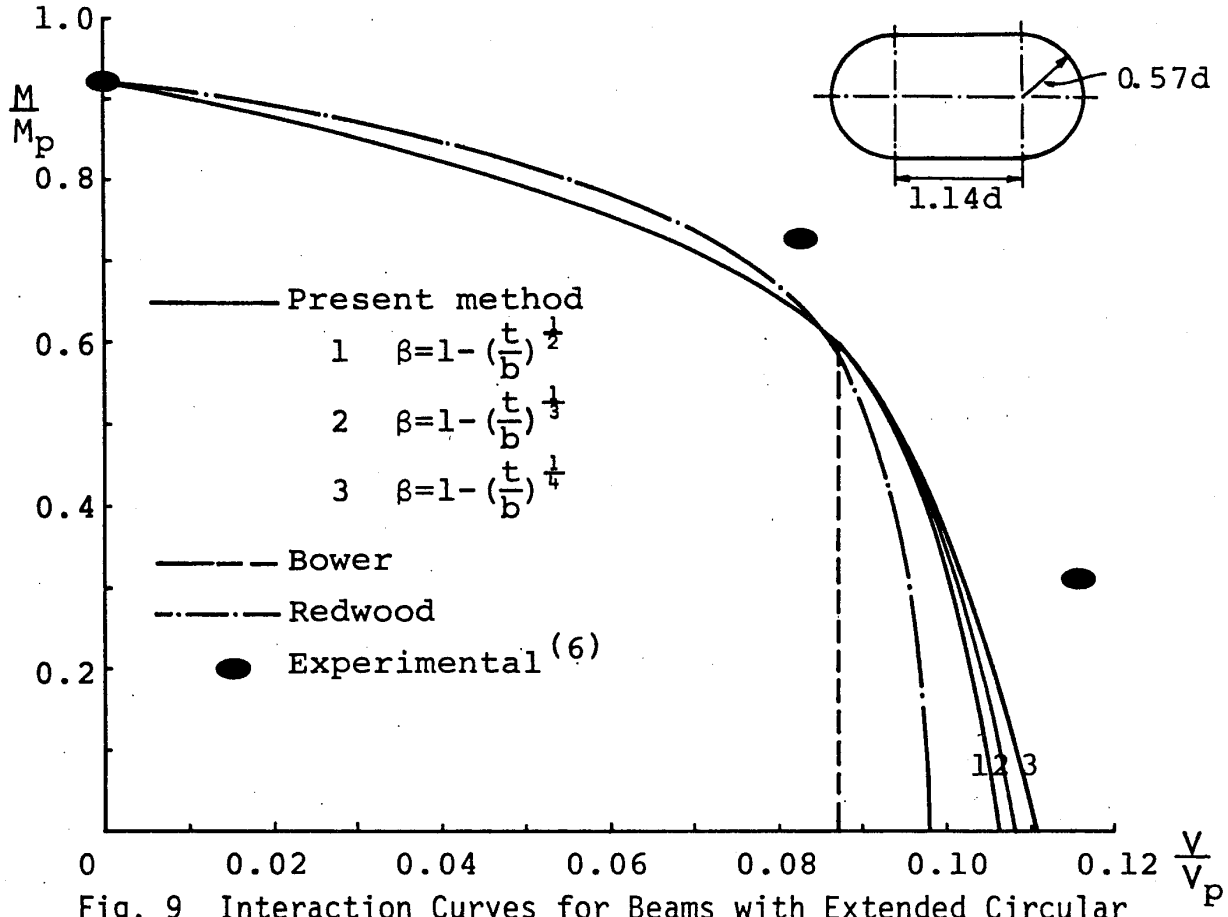

Fig. 9 Interaction Curves for Beams with Extended Circular Holes in Reference (6)

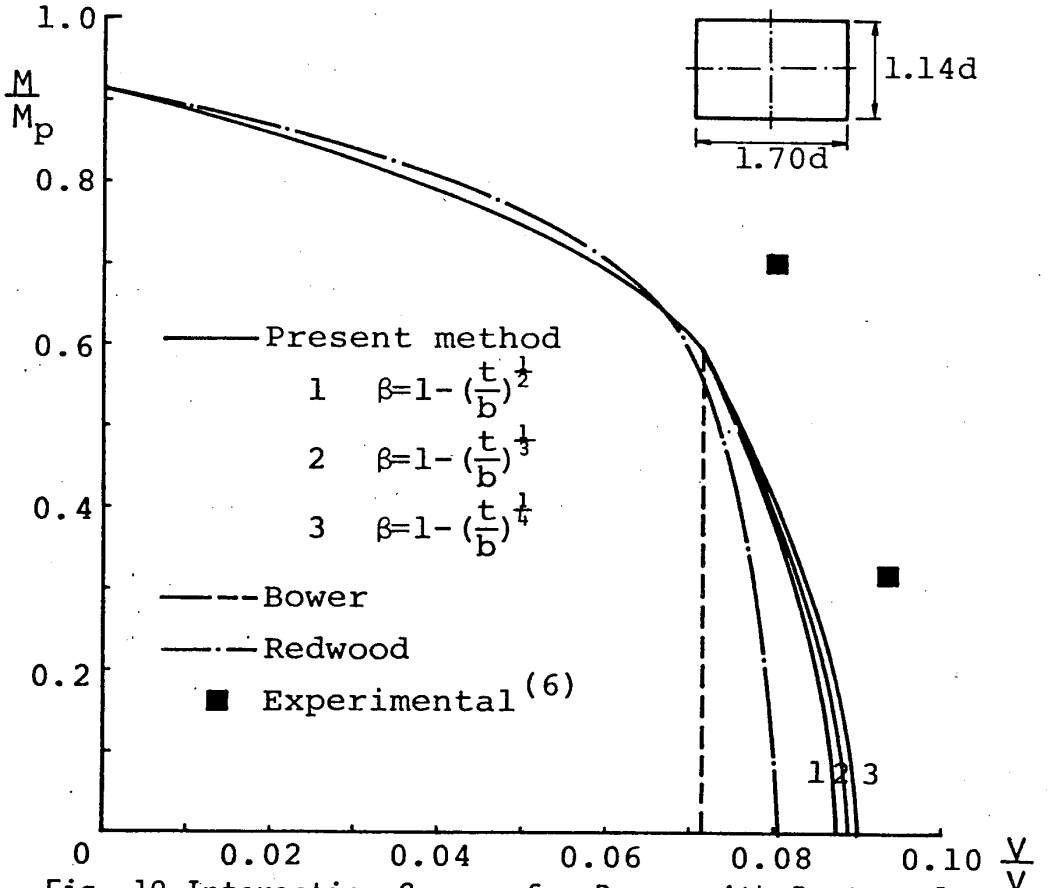

Fig. 10 Interaction Curves for Beams with Rectangular Holes in Reference(6)

The three different methods are also compared to other test results[6] on Fig. 8 to 10. The conservatism of the present method, using Eq. 22 for the parameter β, is within 15 % of the experimental results, and it shows better agreement with the experimental results than the other two methods. The difference between the present method and the other two methods is greatest in the case of circular holes, and is less marked in the case of the extended circular or rectangular holes, as shown in Fig. 7 to 10. The reason for this is as follows; the critical section of the beam with a circular hole occurs closer to the center of the hole than for the extended circular or the rectangular hole in the same loading condition, therefore the local bending moment in the circular hole is less than in the other cases, in which most of the flange area is yielded by the bending stresses due to the applied moment and local bending. Thus in the case of circular holes it is important to consider the shear force carried in the flanges in order to predict the ultimate strength at high shear to moment ratios.

Summary and conclusions

This investigation has been concerned with estimating the ultimate strength of beams with web holes taking into account the shear forces carried in the flanges in addition to those in the web for high shear to moment ratios at the center of the hole. Three variations of the parameter β have been examined for the prediction of the shear forces carried in the flanges. These theoretical results have been compared with the experimental ones, and the following points summarise the conclusions reached:

1. It is necessary to consider the shear forces carried in the flanges in addition to those in the web in order to more accurately estimate the ultimate strength of beams with web holes at high shear to moment ratios. This is especially so for the case of circular holes, in which both Bower's and Redwood's methods show

considerable degrees of conservatism.

2. The theoretical predictions of the present method using the parameter $\beta = 1-(t/b)^{\frac{1}{4}}$ are from 2.4 % to 16.4 % smaller than the experimental values except for r/d = 0.3 in Test No. 4 in which the prediction is 9.4 % greater.

3. Further investigation of the parameter β, including, for example, other factors such as the flange thickness and the web height in the tee-sections, may result in additional improvement of the theoretical prediction.

Appendix 1 - References

1. Redwood, R. G., "Design of Beams with Web Holes," Canadian Steel Industries Construction Council, Willowdale, Ontario,Canada, 1973.
2. Bower, J. E., "Design of Beams with Web Openings", Journal of the Structural Division, ASCE, Vol. 94, No. ST3, Proc. Paper 5869, March, 1968, pp. 783-807.
3. Bower, J. E., "Ultimate Strength of Beams with Rectangular Holes", Journal of the Structural Division, ASCE, Vol. 94, No.ST6, Proc. Paper 5982, June, 1968, pp. 1315-1377.
4. Redwood, R. G., "The Strength of Steel Beams with Unreinforced Web Holes", Civil Engineering and Public Works Review, London, Vol. 64, No. 755, June, 1969, pp.559-562.
5. Congdon, J. G. and Redwood, R. G., "Plastic Behavior of Beams with Reinforced Holes", Journal of the Structural Division, ASCE, Vol. 96, No.ST9, Proc. Paper 7561, Sept., 1970,pp. 1933-1956.
6. Redwood, R. G. and McCutcheon, J. O., "Beam Tests with Unreinforced Web Openings", Journal of the Structural Division, ASCE, Vol. 94, No. ST1, Proc. Paper 5706, Jan., 1968, pp. 1-17.

Apendix II - Notation

The following symbols are used in this paper:

b = width of flange;

$c_1 \sim c_4$ = coefficients defined in Eqs. 16 to 19;

d = half depth of beam;

h = lengrh of web stem at plastic hinge section;

k_1, k_2 = stress reversal coefficients;

M = moment;

M_p = plastic moment of gross beam section;

p = thickness of flange;

r = radius of circular hole;

t = thickness of web;

u = distance from center of hole to plastic hinge section;

v = distance from neutral axis to hole edge at plastic hinge section;

V = shear force;

V_p = maximum shear force carried by gross section of beam;

α = ratio of stress in flange to stress in web $(\sigma_{yf}/\sigma_{yw} = \sigma_f/\sigma_w = \tau_f/\tau_w)$;

β = parameter defining portion of stress combined bending with shear in flange;

σ = normal stress;

σ_f, σ_w = normal stress in flange and web;

σ_{yf}, σ_{yw} = yield stress in flange and web;

τ = shear stress;

τ_f, τ_w = shear stress in flange and web; and

τ_{yf} = shear yield stress in flange.